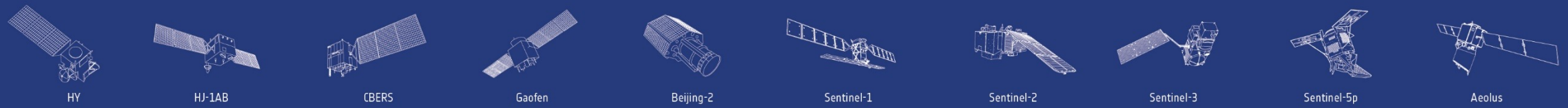

2023 DRAGON 5 SYMPOSIUM

3rd YEAR RESULTS REPORTING

11-15 SEPTEMBER 2023

EMPAC (ID. 59013)

Exploitation of satellite remote sensing to improve our understanding of the Mechanisms and Processes affecting Air quality in China

Dragon 5 3rd Year Results Project

13 SEPTEMBER 2023, 11:00AM - 11:45AM CEST

ID. 59013

PROJECT TITLE: EMPAC

PRINCIPAL INVESTIGATORS: Jianhui Bai (CAS-IAP), Ronald van der A (KNMI)

CO-AUTHORS: Sarah Safieddinne (LATMOS), Yong Xue (Univ. Derby), Costas Varotsos (Univ. Athens), Gerrit de Leeuw (KNMI), Yan Yin (NUIST), XingYing Zhang (NSMC), Kai Qin (CUMT), Zhengqiang Li (AIR-CAS), Jianping Guo (CAMS)

PRESENTED BY: Ronald van der A

EO Data Delivery

Data access (list all missions and issues if any). NB. in the tables please insert cumulative figures (since July 2020) for no. of scenes of high bit rate data (e.g. S1 100 scenes). If data delivery is low bit rate by ftp, insert “ftp”

ESA /Copernicus Missions	No. Scenes
1. OMI	
2. HIMAWARI	
3. MODIS (TERRA&AQUA)	
4. METOP	
5.	
6.	
Total:	
Issues:	

ESA Third Party Missions	No. Scenes
1. Sentinel 3 SLTSR	
2. Sentinel-5P TROPOMI	
3. Sentinel 5	
4. AEOLUS	
5.	
6.	
Total:	
Issues:	

Chinese EO data	No. Scenes
1. FY-3C MERSI	
2. FY-3A/B/C TOU	
3.	
4.	
5.	
6.	
Total:	
Issues:	

Dragon 5 3rd Year Results Reporting

Project's objectives:

- Exploitation of satellite remote sensing to improve our understanding of the Mechanisms and Processes affecting Air quality in China

Results after 3 years of activity:

- CO trend in China
- Mechanisms for changes in O_3 concentration in a subtropical coniferous forest
- Trace gas removal in ice particles and solid particles
- NOx emissions derived from TROPOMI (S5p)
- Meteorological and anthropogenic induced changes in the AOD

Young scientist results:

- Analysis of drone observations of NO2 in the boundary layer.
- Ship emissions on inland rivers
- Arctic lightning NOx

China Air Pollution Prevention and Control Action Plan: the effect on carbon monoxide during [2008-2022]

Selviga Sinnathamby and Sarah Safieddine, LATMOS, CNRS, Sorbonne University, France

IASI **(Infrared Atmospheric Sounding Interferometer)** is a nadir-looking Fourier-Transform Spectrometer that measures Earth's radiance in the thermal infrared range.
Since 2007, three IASI instruments have been embarked on board the polar orbiting meteorological satellites Metop-A, -B and -C.

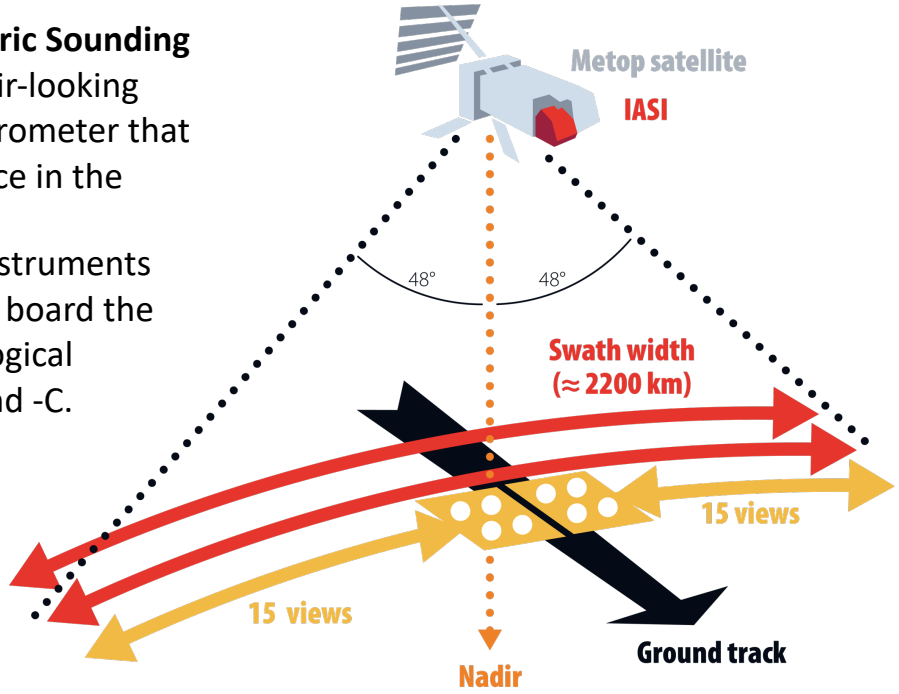

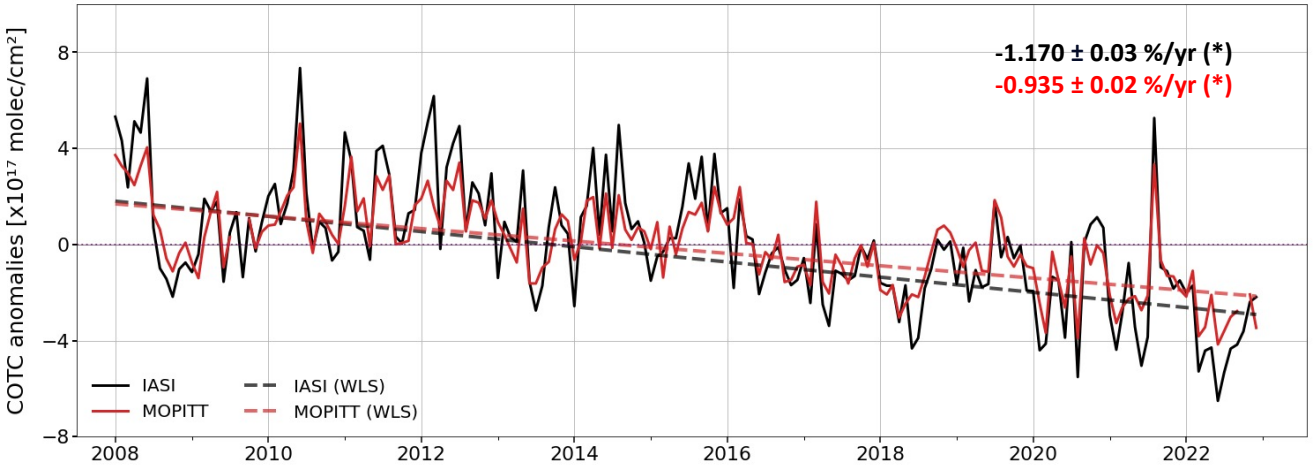

Trends obtained with IASI in the Northeastern region of China (black box) are compared to MOPITT trends. Significant trends to one standard error are marked by an asterix (*).

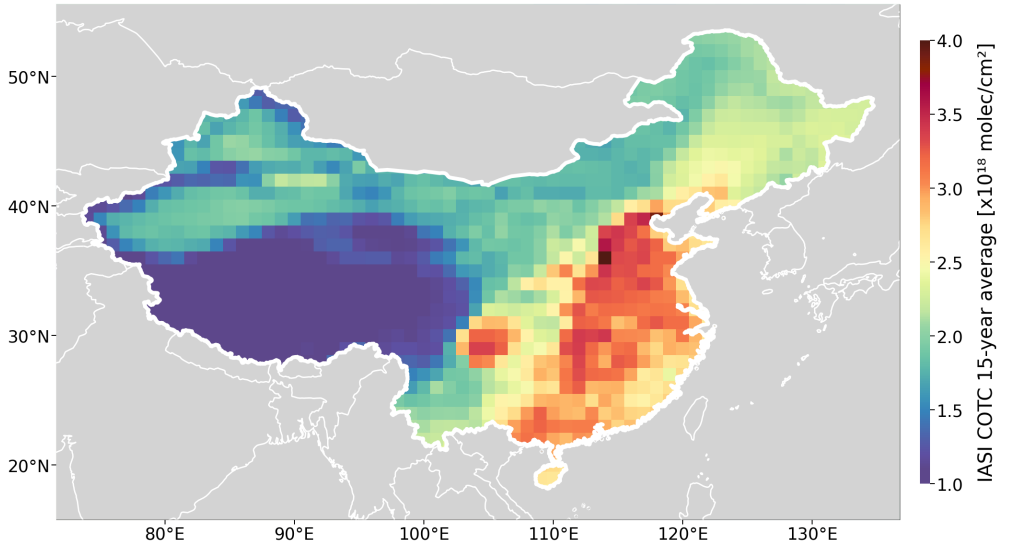

Trend values are estimated by using the *Weighted Least Squares* linear regression, where we define the monthly variance of CO concentrations as weights.

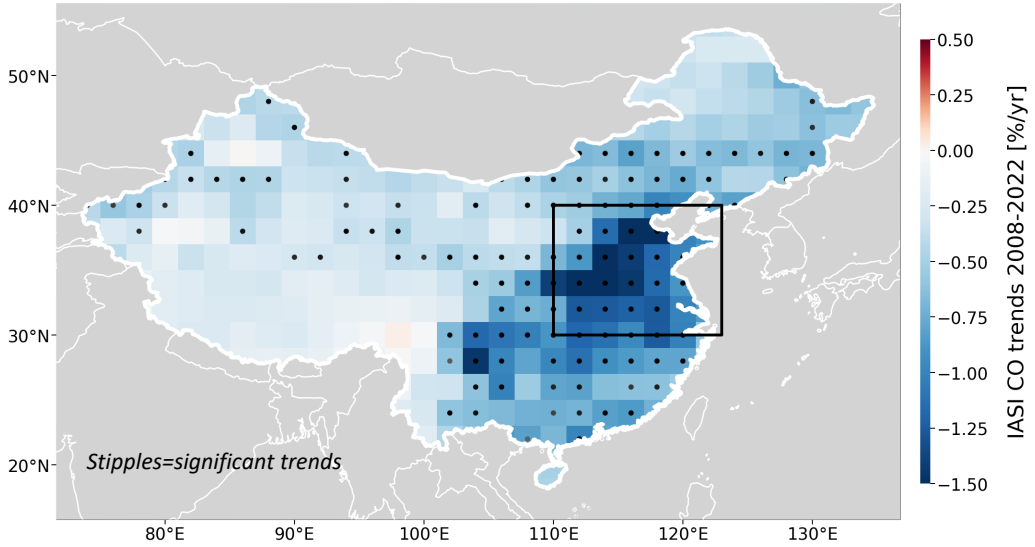

Long-term variations of global solar radiation in Sodankyl*ä*, Antarctic

* **Empirical model of global solar radiation (G):** considering the absorption and scattering roles of atmospheric substances with better simulations

$$G = A_1 e^{-kWm} \times \cos Z + A_2 e^{-S/G} + A_0 \qquad (1)$$

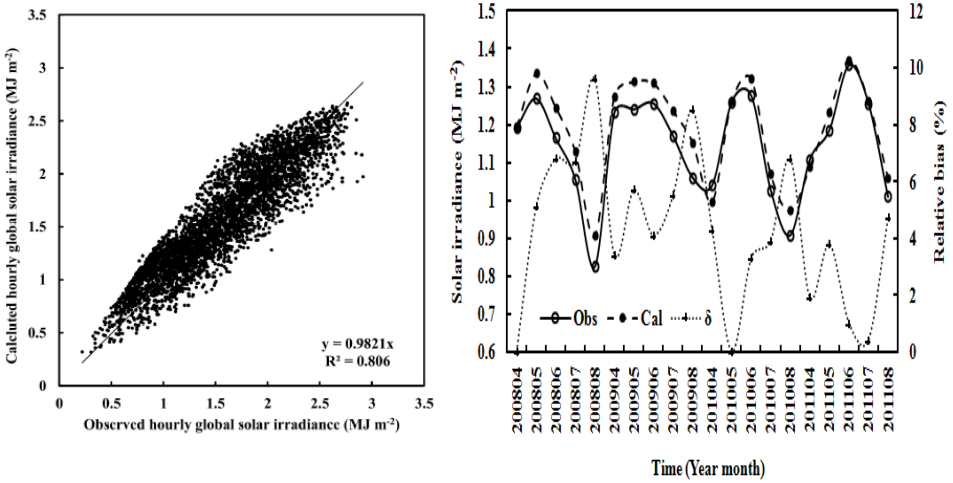

Fig. The calculated and observed global solar radiation during 2008-2011 at Sodankyl*ä* station (n=3962).

Relative bias and RMSE (MJm^{-2}) were 12.8% and 0.22 for hourly G;

Relative bias was 4.3% for monthly G.

- **The empirical model can simulate G at the top of the atmosphere (TOA)** using $A_1+A_2+|A_0|$. The ratios of G to solar constant were 6.4% -11.2% (S/G: ≤0.1 - ≤ 0.8)
- **Losses of G caused by absorbing and scattering substances (G_{LA}, G_{LS}), total loss (G_L)**

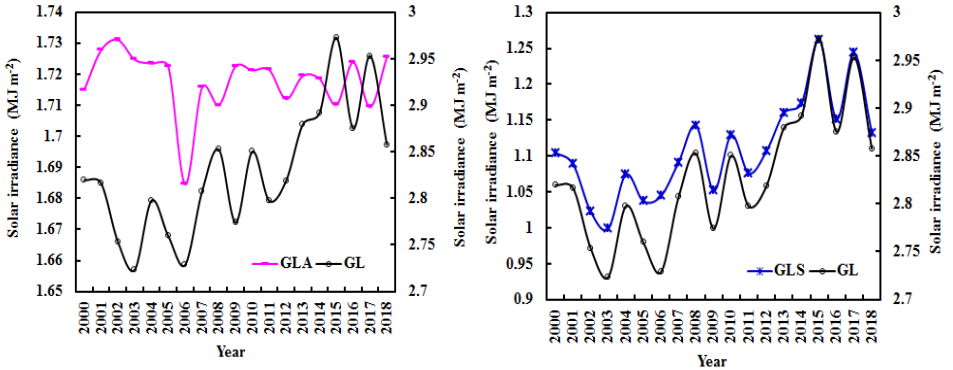

- **G_{LA} and G_{LS}:** decreased by 0.01% and increased by 0.88%; **G_L** increased by 0.32% per year in 2000 - 2018

Fig. Annual losses of G in the atmosphere under all sky conditions

- **Annual air temperature increased 0.07 ℃, which was contributed by the increases of G_{LS} and G_L.** Water vapor and S/G increased by 0.28% and 1.6% per year, respectively in 2000 - 2018

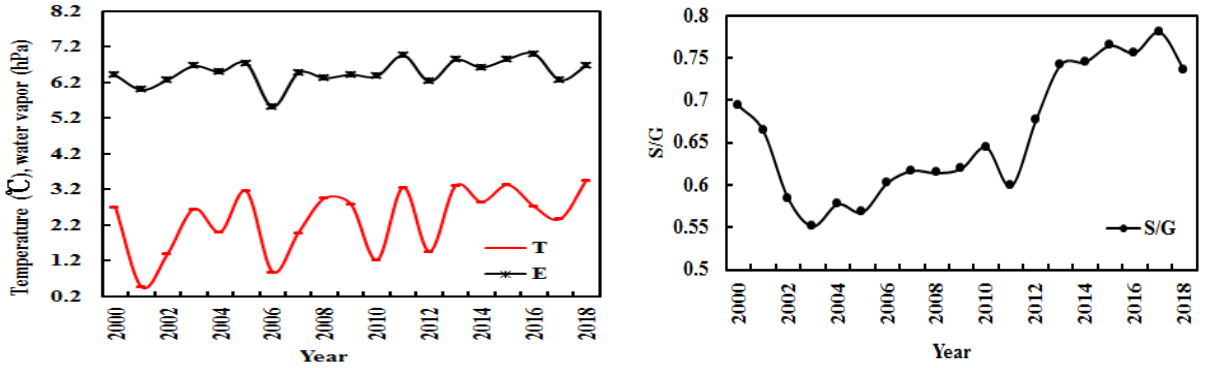

Fig. Annual air temperature, water vapor pressure (E) and scattering factor (S/G)

- **Empirical model can calculate the albedos at the surface and the TOA**, which were in reasonable agreements with the corresponding satellite retrievals

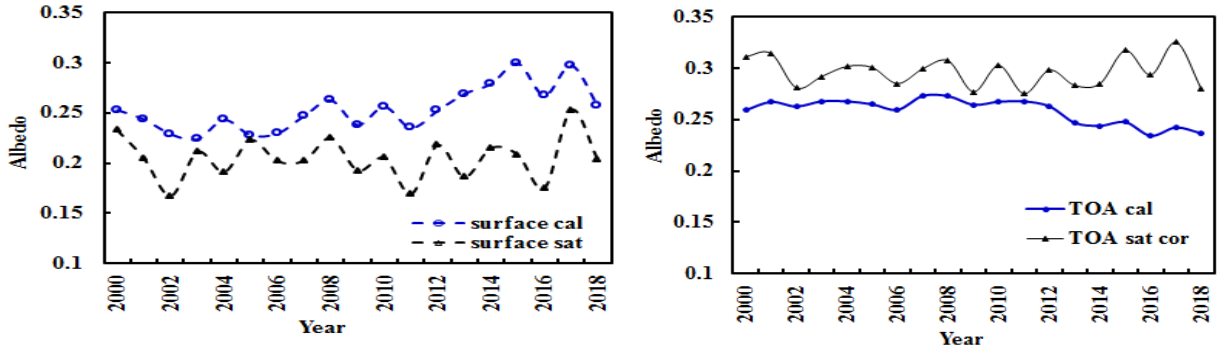

Fig. Calculated and satellite retrieved annual albedos at the surface and the TOA averaged from April to September

- **Conclusion** An empirical model of global solar radiation was developed and used to calculate global solar radiation and its losses in the atmosphere as well as albedos. Their long-term variations together with air temperature and scattering factor S/G were fully studied. In 2000-2018, the calculated and observed G at the surface decreased; the albedos increased at the surface, but decreased at the TOA.

On the tropospheric gases removal due to their diffusion in ice particles

Costas VAROTSOS* and Yong XUE**

*Department of Environmental Physics and Meteorology, National and Kapodistrian University of Athens, Athens 15784 Greece

**School of Environment Science and Spatial Informatics, University of Mining and Technology, Xuzhou, Jiangsu 221116, PR China

When in a solid a single diffusion mechanism is operative, the diffusion coefficient, D, is often found to obey an Arrhenius type behaviour, i.e $D = D_0 \exp[-E/(k_B T)]$

Summary of rate parameters for the diffusion coefficients of selected compounds in ice.

	E(kcal/mol)	D_o (cm^2/s)	D(180 K) (cm^2/s)	T(K) Ref.
HCl	15.3±1.0	$1.5\times10^{7\pm0.2}$	4.83×10^{-12}	169.0–194.9; Livingston et al., 2001
HCOOH	21.8±0.9	$8\times10^{14\pm0.1}$	2.42×10^{-12}	175.1-194.9; Livingston et al., 2002
CH_3COOH	17.0±0.7	$1.0\times10^{10\pm0.1}$	2.08×10^{-11}	169.9–194.9; Livingston et al., 2002
	13.14±3.0	$0.813\times10^{6\pm3.2}$	8.6×10^{-11}	198–213; Nehme, 2006
CH_3OH	15.2±0.7	$2.4\times10^{7\pm0.3}$	7.8×10^{-12}	169.4-185.4; Livingston et al.,2002

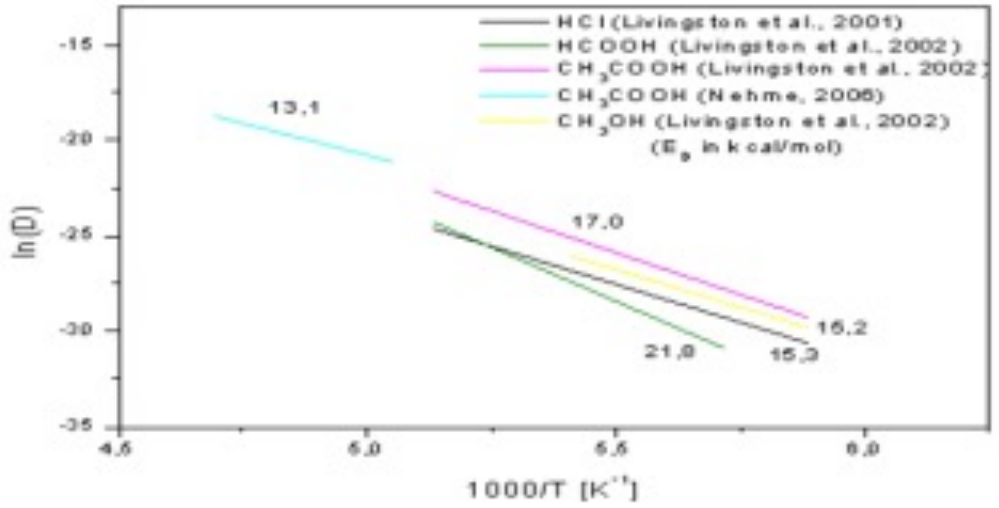

Fig. 1. Arrhenius plots for temperature dependent diffusion coefficients for various species in ice as obtained by the LRD depth-profiling technique (Livingston et al., 2001, 2002) and chemical titration (Nehme, 2006). The figures on the individual lines are activation energies (in kcal/mol) as derived by the authors.

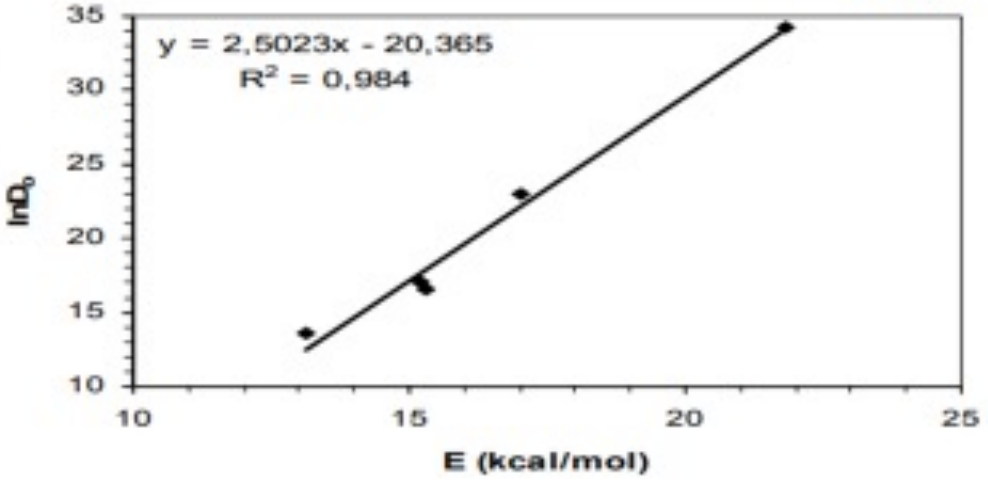

Fig. 2. Relationship between the pre-exponential factor D_o of the diffusion coefficient and the activation energy E.

CONCLUSIONS

From Figures 1 an2 it is argued that the diffusion in ice of these compounds is governed by a vacancy – mediated mechanism, i.e., H2O vacancies are required to diffuse to lattice sites adjacent to these compounds prior to the diffusion of the corresponding molecule into the vacancy sites. In addition, we show that the diffusion coefficients of these compounds exhibit a specific interconnection, i.e., a linear relationship holds between the logarithm of the pre-exponential factor, *Do*, and the activation energy *E*. Based on this conclusion we also calculated the tropospheric O3 removal due to its diffusion in solid particles (e.g., dust and black carbon particles or in cirrus clouds).

Application: *Materials' Deterioration from air pollution and Aerosols*

remote sensing Published: 20 June 2023 MDPI

Article

Satellite Sensed Data-Dose Response Functions: A Totally New Approach for Estimating Materials' Deterioration from Space

Georgios Kouremadas [1,*], John Christodoulakis [1,2], Costas Varotsos [1] and Yong Xue [3,4]

$$D_{O_3} = 1.1 \times 10^{-6} exp\left(\frac{-1896}{T}\right)$$

$$D_{NO_2} = exp\left[(-1.885) \cdot \left(\frac{1000}{T}\right) + 6.641\right]$$

$$D_{SO_2} = exp\left[(-2.96) \cdot \left(\frac{1000}{T}\right) + 10.42\right]$$

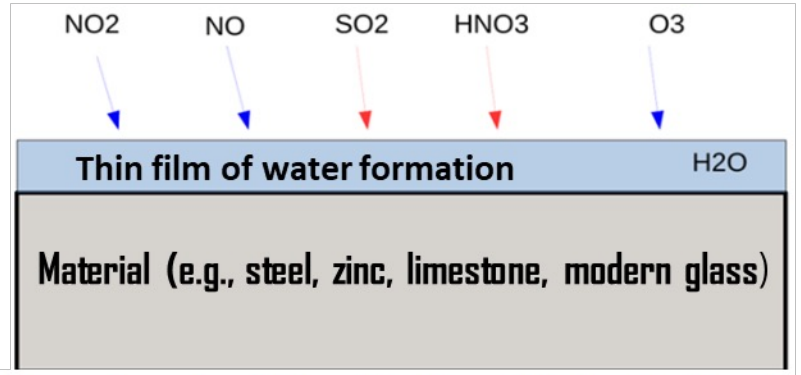

When construction materials are exposed to the atmospheric environment, they are subject to deterioration, which varies according to the time period of exposure and the location. A tool named Dose–Response Functions (DRFs) has been developed to estimate this deterioration. DRFs use specific air pollutants and climatic parameters as input data. Existing DRFs in the literature use only ground-based measurements as input data. This fact constitutes a limitation for the application of this tool because it is too expensive to establish and maintain such a large network of ground-based stations for pollution monitoring.

In this study, we present the development of new DRFs using only satellite data as an input named Satellite Sensed Data Dose-Response Functions (SSD-DRFs). Due to the global coverage provided by satellites, this new tool for monitoring the corrosion/soiling of materials overcomes the previous limitation because it can be applied to any area of interest. To develop SSD-DRFs, we used measurements from MODIS and AIRS on board Aqua and OMI on Aura. According to the obtained results, SSD-DRFs were developed for the case of carbon steel, zinc, limestone, and modern glass materials. SSD-DRFs are shown to produce more reliable corrosion/soiling estimates than "traditional" DRFs using ground-based data. Furthermore, research into the development of the SSD-DRFs revealed that the different corrosion mechanisms taking place on the surface of a material do not act additively with each other but rather synergistically.

for carbon steel

		RH	RH * NO_2	RH *AOD	RH^2 * NO_2 * SO_2
Mass loss	Pearson Correlation	0.498 **	0.443 **	0.611 **	0.484 **
	N	110	110	110	110

** Correlation is significant at the 0.01 level (2-tailed).

for zinc

		RH	RH * O_3	RH * SO_2
Mass loss	Pearson Correlation	0.383 **	0.386 **	0.232 *
	N	112	112	112

** Correlation is significant at the 0.01 level (2-tailed). * Correlation is significant at the 0.05 level (2-tailed).

for limestone

		RH	RH * NO_2	RH * AOD
Mass loss	Pearson Correlation	0.234 *	0.202 *	0.127
	N	105	105	105

* Correlation is significant at the 0.05 level (2-tailed).

modern glass

		Temp	AOD	SO_2 * D_{SO2}	NO_2 * D_{NO2}	O_3 * D_{O3}
Soiling	Pearson Correlation	0.612 **	0.465 **	0.434 **	0.360 **	0.586 **
	N	97	97	97	97	97

** Correlation is significant at the 0.01 level (2-tailed).

Time series and trends:
Satellites tell you: How China's Air Pollution Has Changed in the Past Two Decades

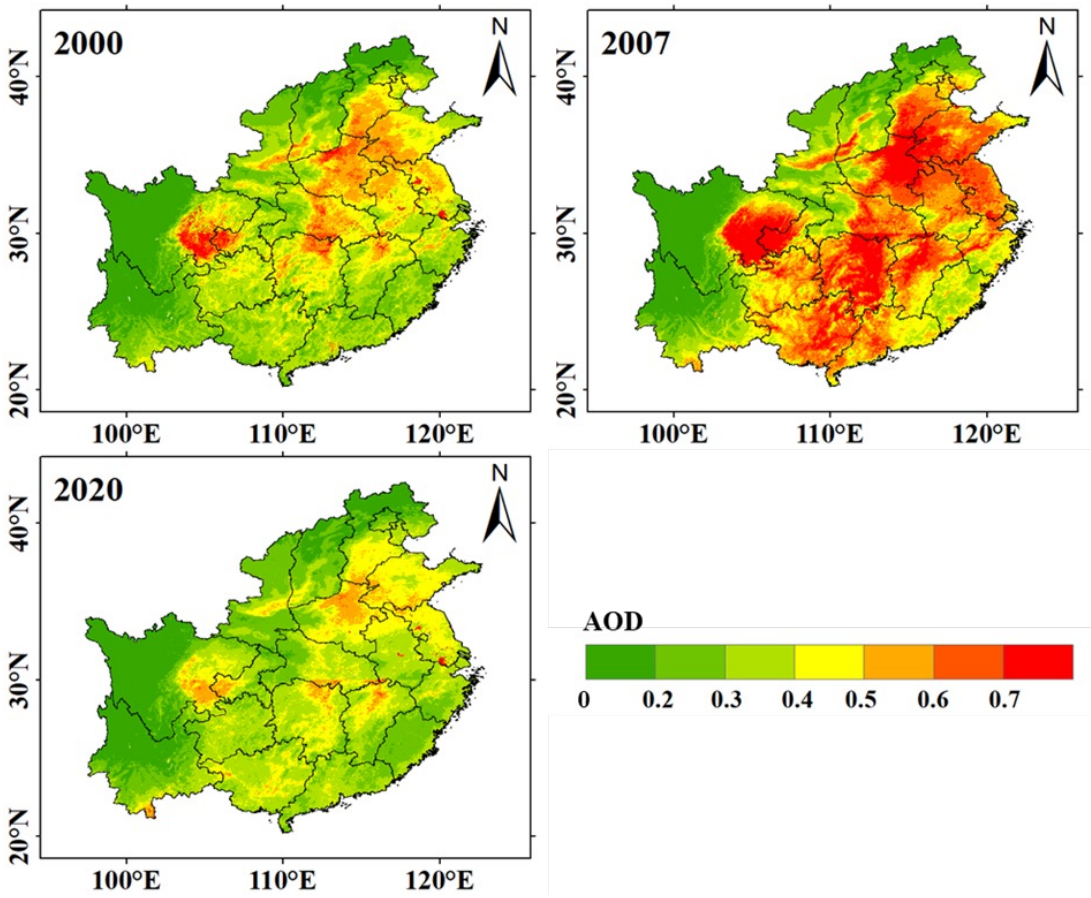

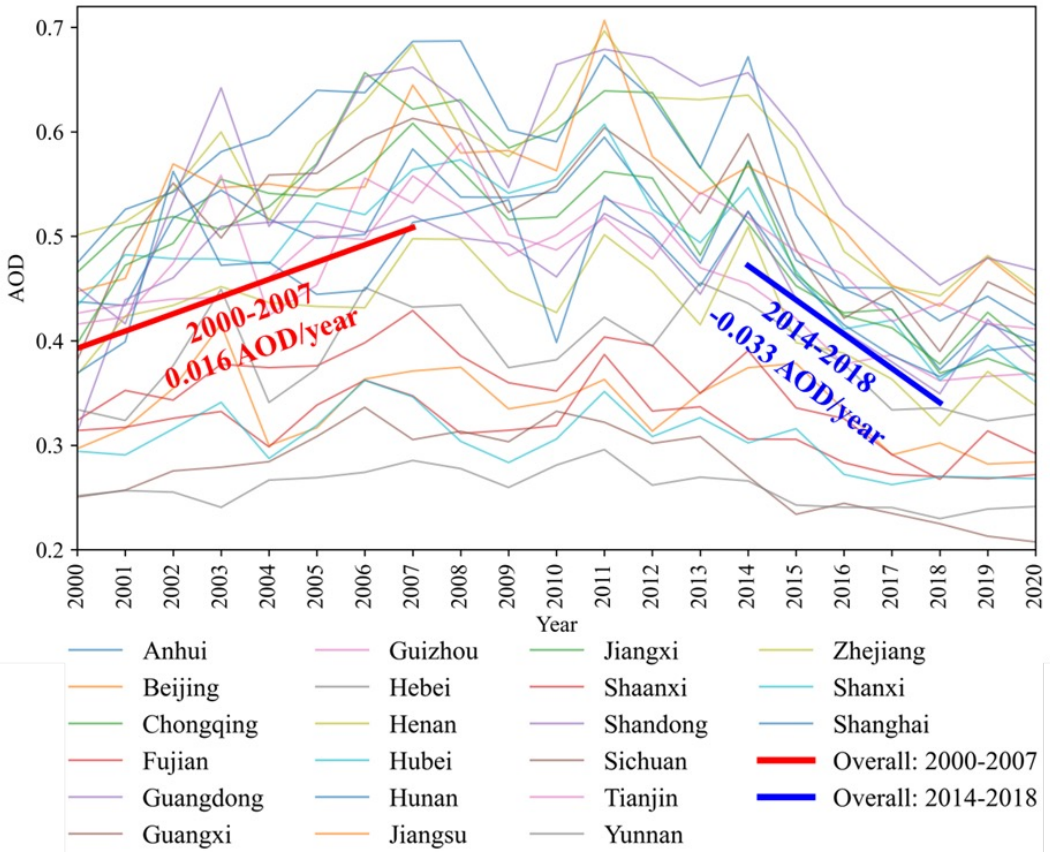

Annually averaged Satellite-derived AOD maps over SE China and provincial scale time series show the increase of AOD between 2000 and 2007. The strong decrease after 2014 shows the effectiveness of emission reduction policy, resulting in overall lower AOD in 2020 than in 2000!

Zhengqiang Li, Gerrit de Leeuw, Xiaoxi Yan, Cheng Fan, Ying Zhang:
Satellites Tell You: How China's Air Pollution Has Changed in the Past Two Decades. China Focus, September 2023
(AirCAS/KNMI cooperation)

NOx emissions using TROPOMI

DECSO version 6.1 using superobservations based on the TROPOMI NO2 retrieval v.2 (PAL data set) and the latest version of CHIMERE (version 2020r3).

Spatial resolution: 10 km

Temporal resolution: daily

Year: 2019

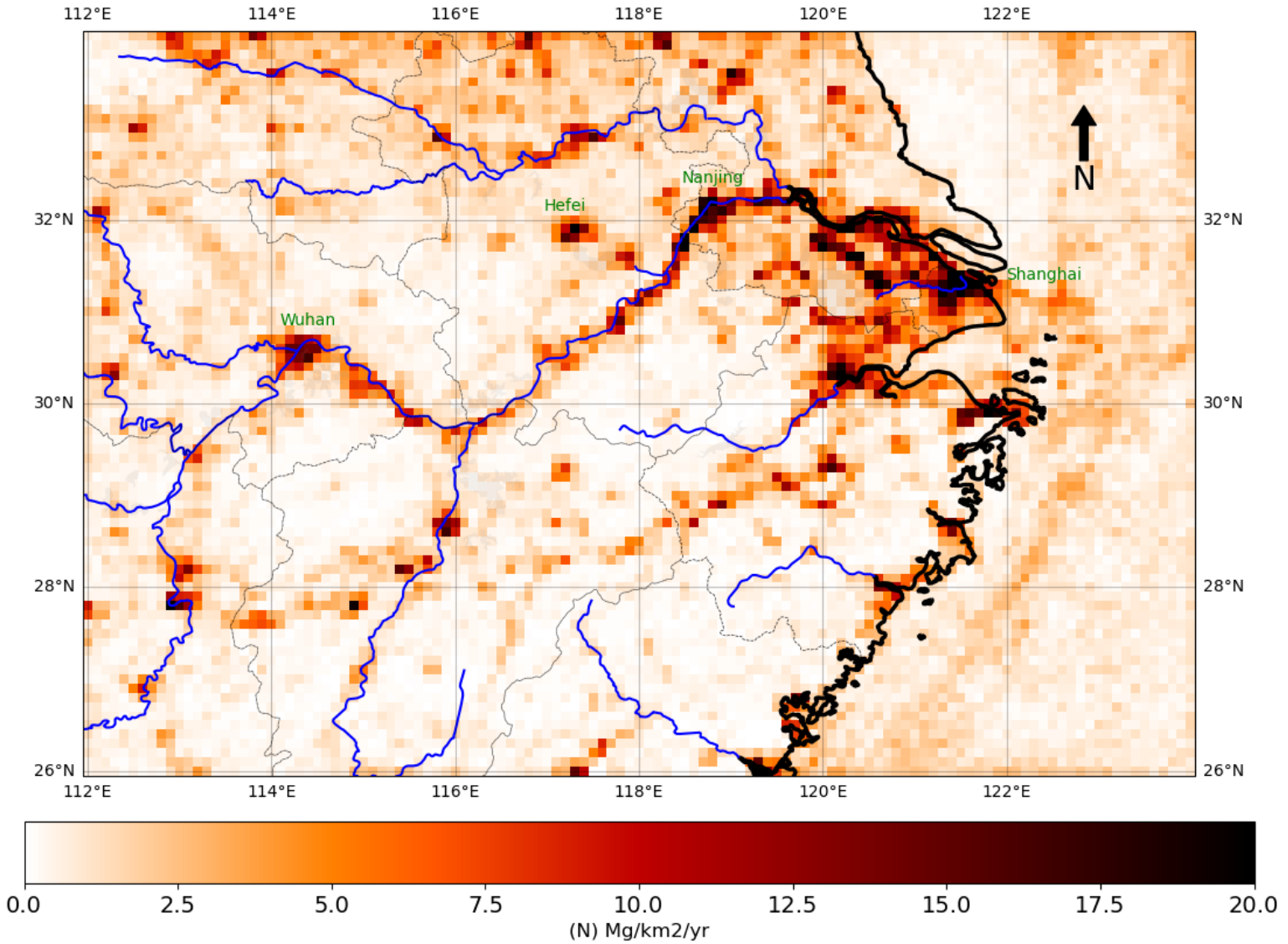

For boundary layer research in Nanjing: see poster (ID 281) of Mirjam den Hoed

For ship emissions from the Yangtze river: see poster (ID 200) of Xiumei Zhang

Young scientists

Europe

- Mirjam den Hoed (KNMI). Travelling to China was complicated for a while, therefore no new campaign has been joined. She is currently analysing data from an earlier (pre-covid) campaign, which she participated.

China

- Xin Zhang (NUIST): he has stayed at KNMI from October 2021 – September 2022 to use TROPOMI observations to study Arctic source, in particular lightning.
- Xiumei Zhang (NUIST): she has stayed at KNMI for one year (March 2022-March 2023), to study ship emissions in the Yangtze River Delta and in the Rotterdam region using AIS and satellite data. She is now measuring ship emissions at Nanjing using a MAX-DOAS instrument.

Chinese Young scientists contributions in Dragon 5

Name	Institution	Poster title	Contribution including period of research
Xin Zhang	NUIST, Nanjing	N/A	Lightning NO2 in the arctic 2020-2023 (PhD obtained in 2023)
Xiumei Zhang	NUIST, Nanjing	Analysis of Emissions based on AIS and MAX-DOAS observations	Inland ship emissions 2020-2023

Lightning NO_2 in the Arctic

Consecutive TROPOMI observations for tracking lightning NO_2 in the Arctic

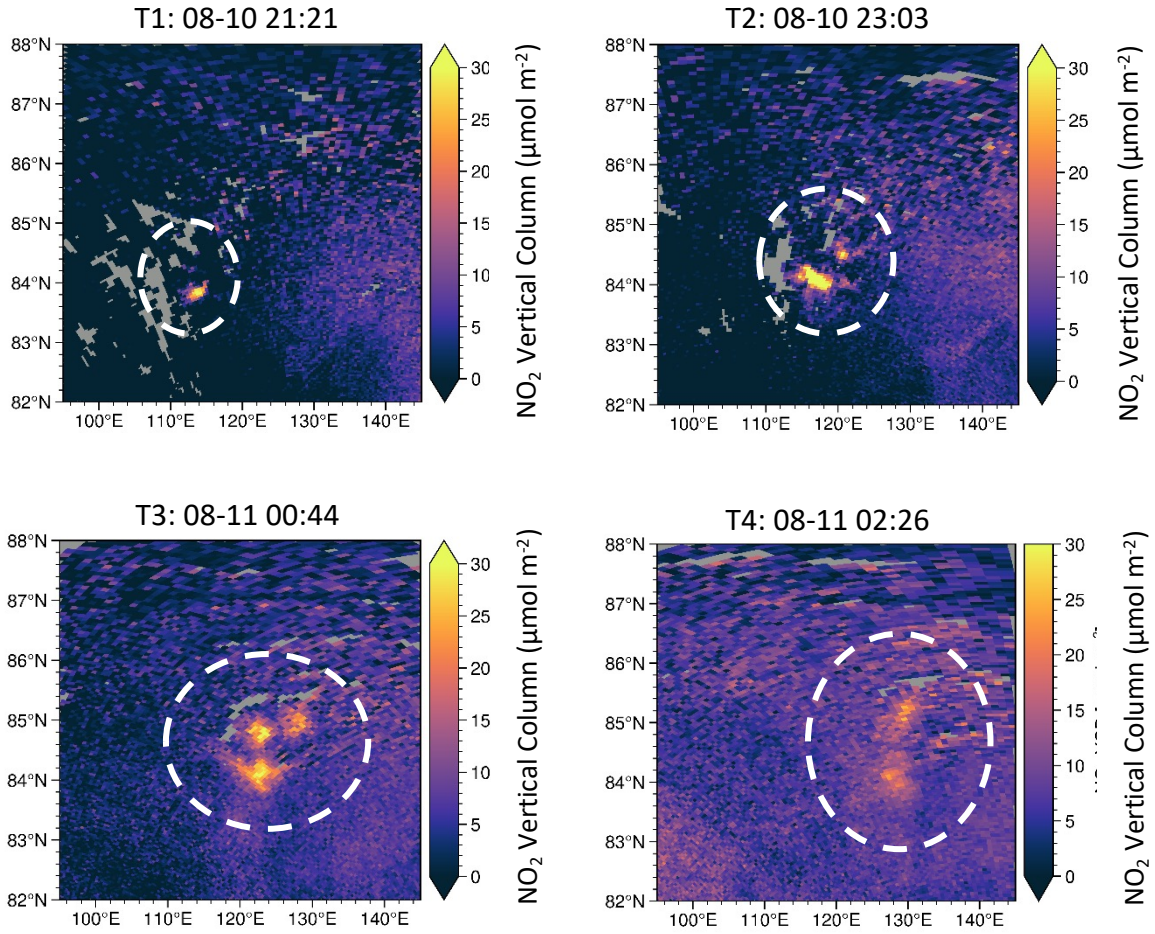

Zhang et al. (2023), ES&T

Extraction of lightning NO_2 pixels

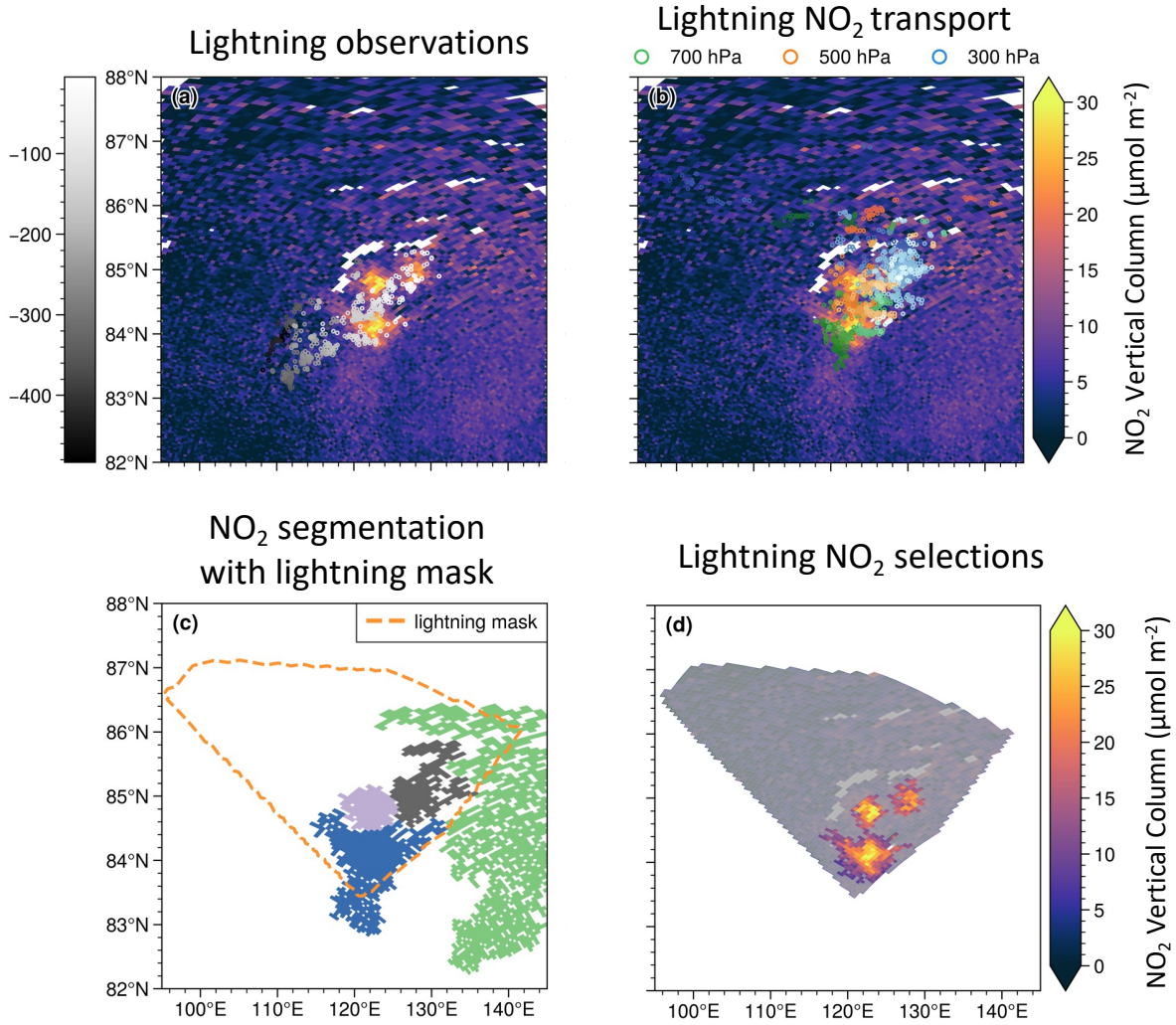

Lightning NO_2 in the Arctic

Short-term (hourly scale)

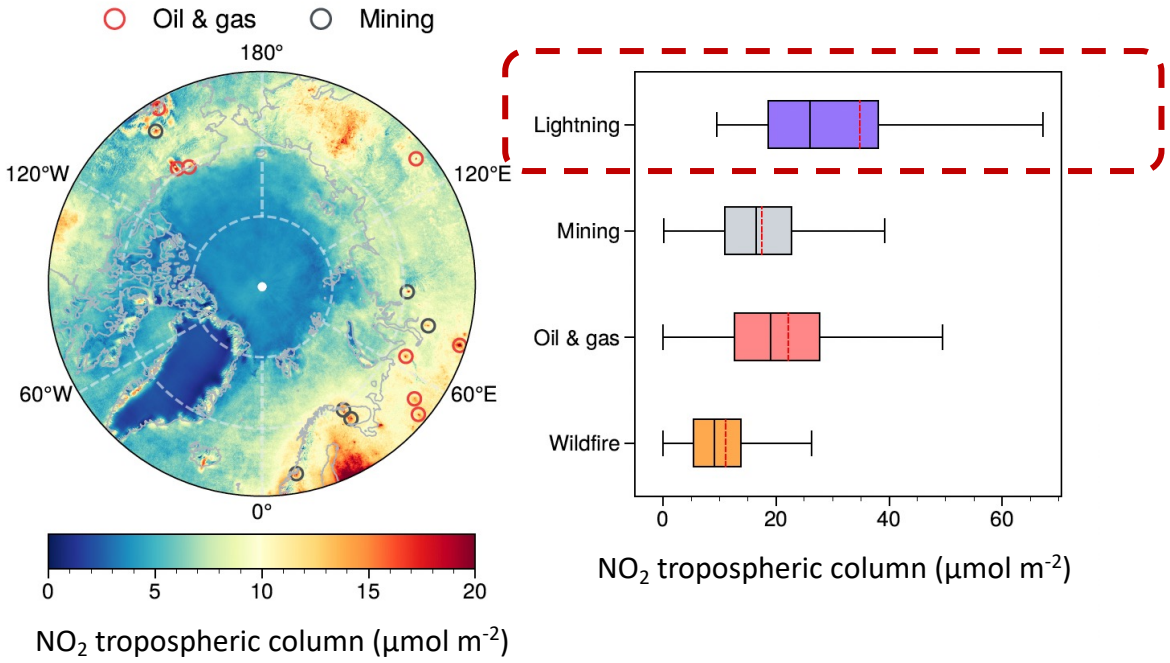

Lightning NO_2 is **comparable** to anthropogenic NO_2 in the Arctic.

Zhang et al. (2023), ES&T

Long-term (monthly scale)

Anthropogenic NO_x

1160 (ship) + 350 (others) t N/month

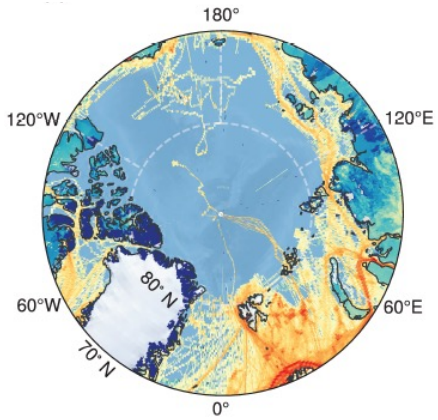

Soil NO_x

2670 t N/month

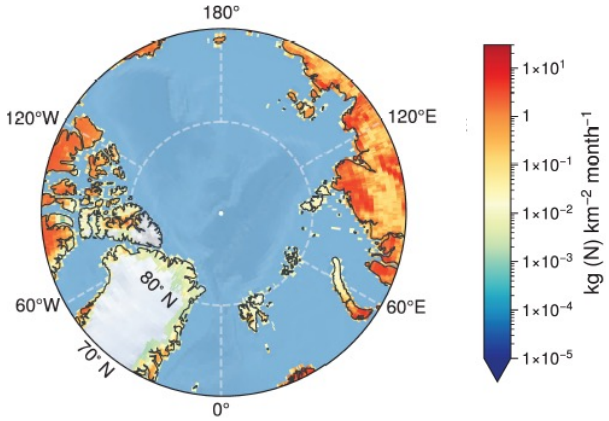

Lightning

73 t N/month

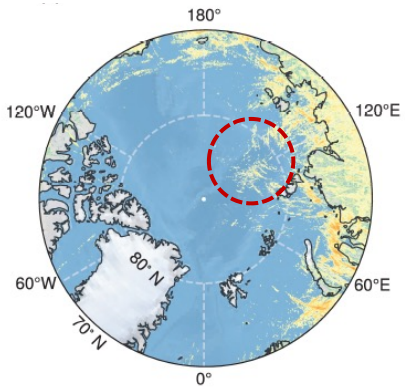

- NO_x emissions over the land:
  soil > anthropogenic > lightning
- NO_x emissions over the ocean
  ship > lightning

Emissions from inland ships on the Yangtze river

Data from AIS signals that we use:

- Type of ship
- Speed
- Size

=> Emissions calculated per ship or per km

AIS signals received at NUIST, Nanjing.

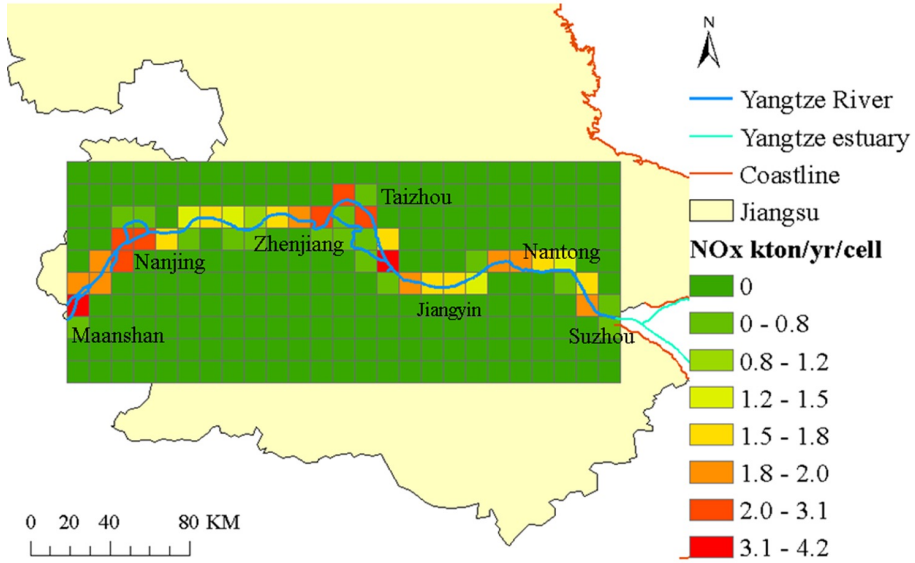

See poster by Xiumei Zhang (#200)

European Young scientists contributions in Dragon 5

Name	Institution	Poster title	Contribution including period of research
Mirjam den Hoed	KNMI, The Netherlands	Comparison of vertical NO2 profiles measured in-situ from a Quadcopter, retrieved from MAX_DOAS observations and computed using the Chimere Chemistry-Transport model	2018-2023

Comparison of in-situ NO_2 drone soundings (~1 km) with MAX-DOAS and CHIMERE

36 calibrated NO_2 vertical profiles (2-12 June 2018)

Diurnal cycle of NO_2 clearly visible:

- Elevated NO_2 concentrations close to the surface during the night and early morning.
- Development of PBL/rise of PBL height from sunrise onward.
- Well mixed PBL/flat NO_2 vertical profile shapes with lower concentrations during afternoon.

Daily NO_2 volume mixing ratios (ppbv) from combined upward and downward soundings averaged over bins of 5 hPa.

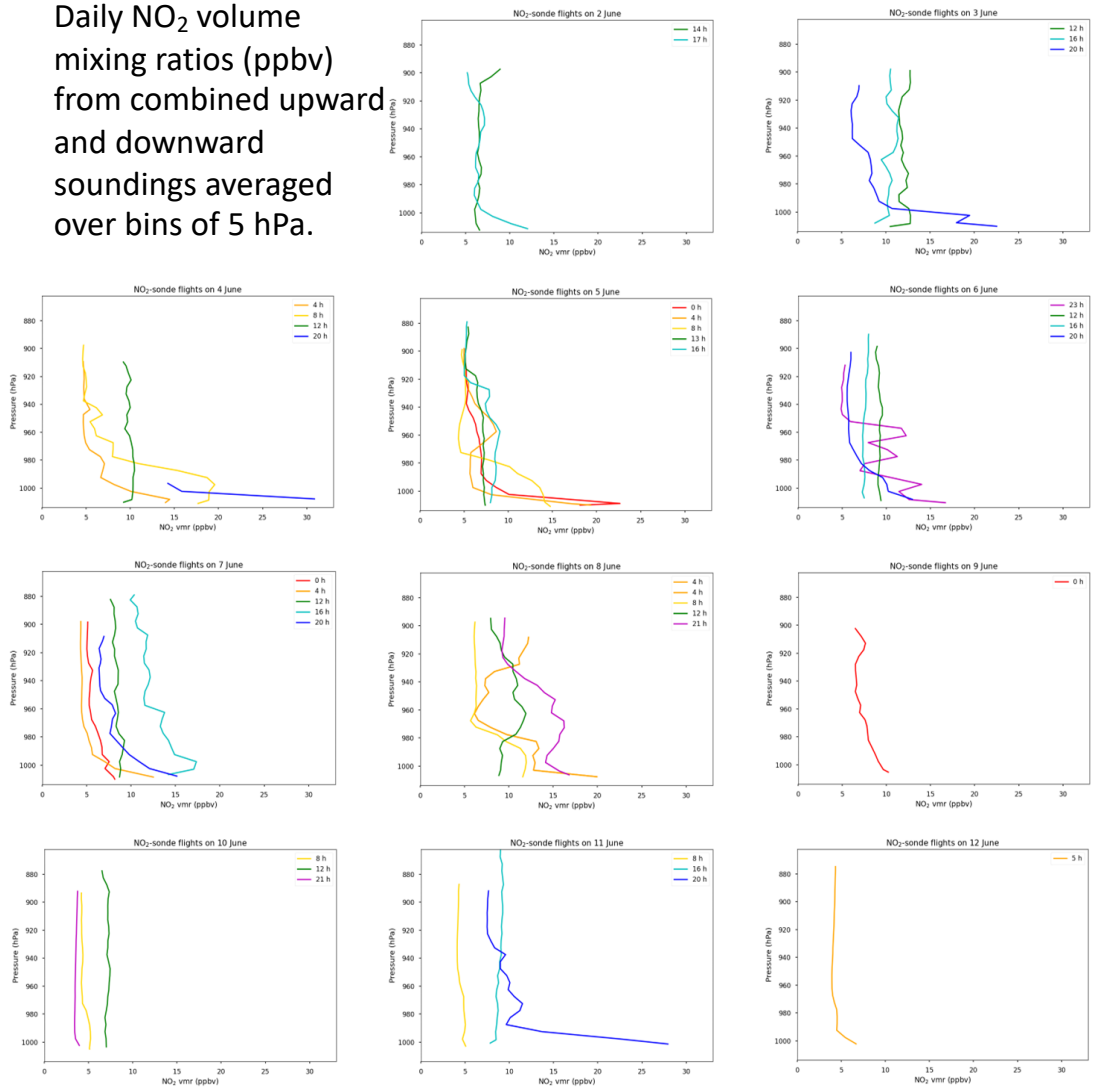

Comparison of in-situ NO_2 drone soundings (~1 km) with MAX-DOAS and CHIMERE

COMPARISON NO2-SONDE & CHIMERE

- **Median absolute NO_2 error is negative:** CHIMERE systematically underestimates the NO_2 vmr for every vertical layer on the drone measurement site. This can be explained by the fact that the modeled vmrs apply to a larger region (0.1°) while NO_2 surface concentrations have a higher spatial variability.
- **More and larger outliers in the lower layers and decreasing IQRs with height** for the NO_2 absolute error: modeled NO_2 vmrs are less accurate closer to the surface where NO_2 is emitted.

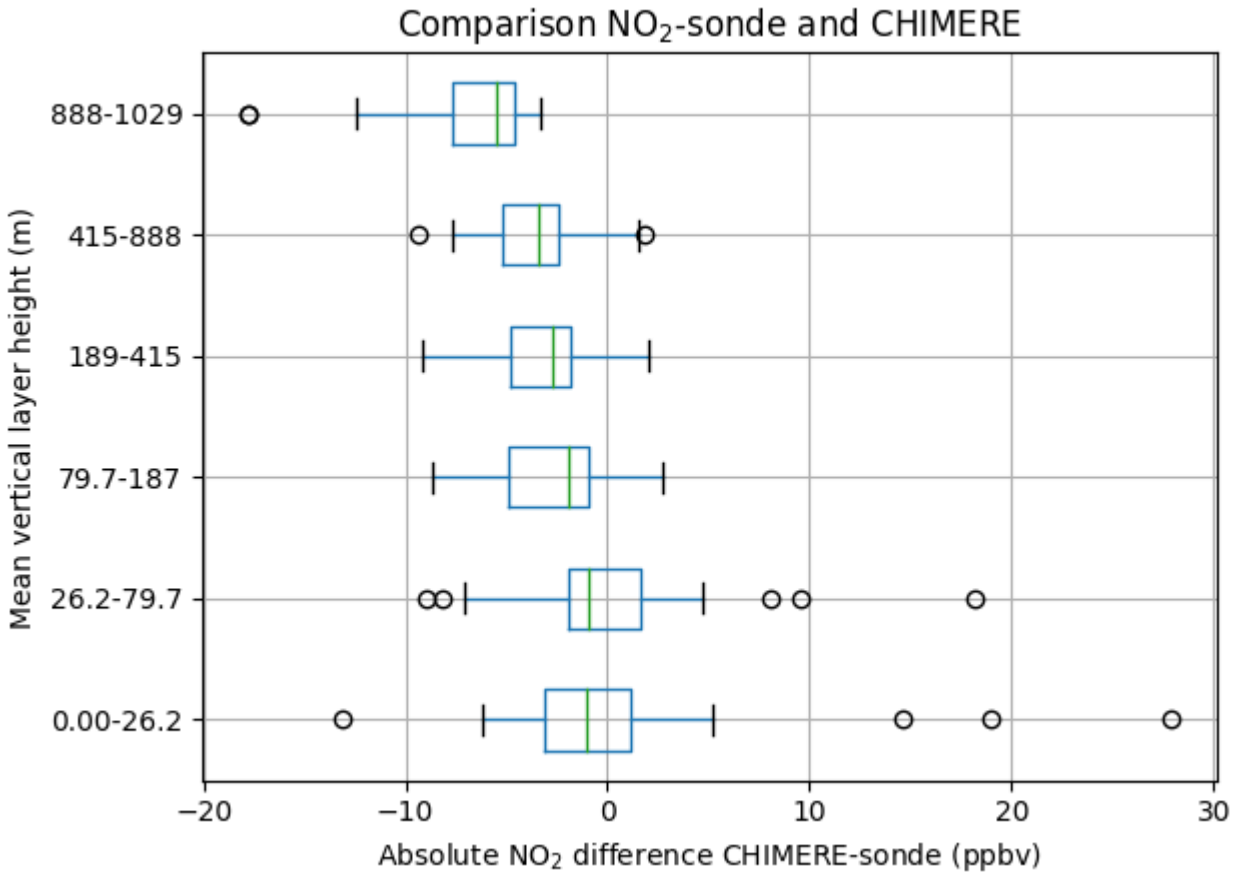

Comparison of in-situ NO_2 drone soundings (~1 km) with MAX-DOAS and CHIMERE

COMPARISON NO_2-SONDE & MAX-DOAS

- Large differences in **relative error** between NO_2-sonde and MAX-DOAS NO_2 column concentrations (molecules·cm^{-3}) ranging from **-89 to 155 %.**
- **3 cases with low relative error (8-15%).** No common contributing factors could be identified. 2/3 were conducted during the weekend (lower local emissions from traffic, industry etc.).
- Effects of **wind direction, wind speed, time, cloud cover not statistically significant.** 13 collocated profiles: insufficient sample sizes.

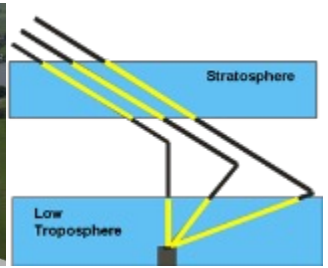

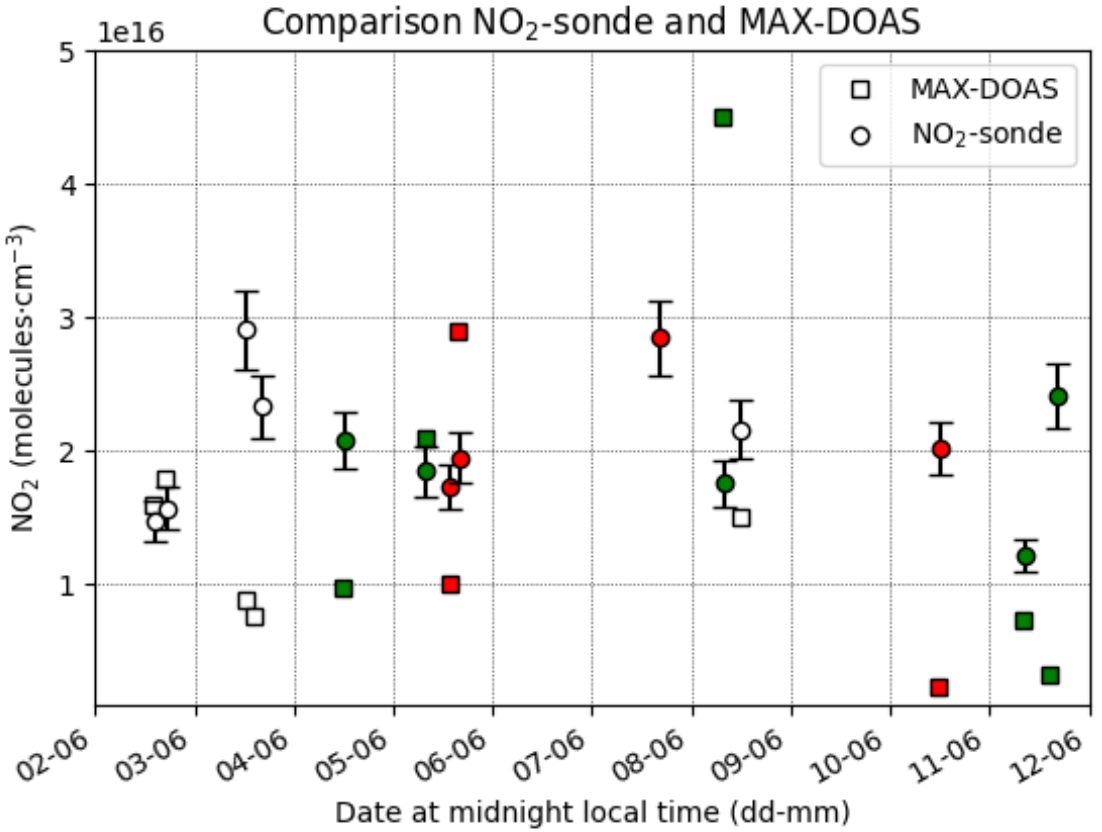

Green: cloud free conditions; Red: low clouds;
White: cloud cover/height unknown